

## Fabrication of Al–La–Ni–Fe Bulk Metallic Glasses by Spark-Plasma Sintering of Mechanically Alloyed Powders

J. S. KIM, O. T. H. NGUYEN, P. P. CHOI, J. C. KIM and Y. S. KWON

Research Center for Machine Parts and Materials Processing, School of Materials Science and Engineering, University of Ulsan, P. O. Box 18, Ulsan 680-749 (South Korea)

E-mail:jskim@mail.ulsan.ac.kr

### Abstract

High-energy ball-milling in hexane medium was employed to prepare amorphous Al–La–Fe–Ni alloys of three different nominal compositions ( $\text{Al}_{82}\text{La}_{10}\text{Ni}_4\text{Fe}_4$ ,  $\text{Al}_{85}\text{La}_9\text{Ni}_3\text{Fe}_3$  and  $\text{Al}_{88}\text{La}_6\text{Ni}_3\text{Fe}_3$ ). Using a planetary ball mill (AGO-2) at a rotational speed of 300 rpm, nearly complete amorphization could be achieved for the  $\text{Al}_{82}\text{La}_{10}\text{Ni}_4\text{Fe}_4$  alloy after milling for 350 h. In contrast, the  $\text{Al}_{85}\text{La}_9\text{Ni}_3\text{Fe}_3$  and  $\text{Al}_{88}\text{La}_6\text{Ni}_3\text{Fe}_3$  samples remained crystalline to a certain extent even after prolonged milling and contained *fcc* Al crystallites. The glass forming ability was found to increase with decreasing Al and increasing La content, which can be ascribed to the enhanced atomic size mismatch of the constituents on La addition. Amorphous  $\text{Al}_{82}\text{La}_{10}\text{Ni}_4\text{Fe}_4$  powder undergoes two-stage crystallization with onset temperatures at 640 and 700 K and glass transition at 566 K. Differences to DSC traces of previously studied melt-spun samples are believed to be mainly due to carbon impurity incorporation and compositional changes during milling. Taking into account the DSC data, consolidation of amorphous  $\text{Al}_{82}\text{La}_{10}\text{Ni}_4\text{Fe}_4$  powder was attempted by means of spark-plasma sintering at a temperature of 613 K and applied pressures of 400 and 600 MPa. Compacts produced under these conditions were found to have relative densities of 80 and 96 %, respectively.

### INTRODUCTION

A number of attempts to produce bulk amorphous alloys by various techniques have been carried out in the last decades. Recently, Al-based amorphous alloys have been attractive materials since they possess outstanding mechanical properties with potentially high corrosion resistance and thermal stability [1]. For example, an amorphous  $\text{Al}_{85}\text{Ni}_7\text{Co}_3\text{Y}_5$  alloy can have tensile strength exceeding 1260 MPa and the tensile fracture strength of an amorphous  $\text{Al}_{87}\text{Ni}_9\text{Fe}_1\text{Ce}_3$  alloy containing nanoscale Al particles can amount up to 1560 MPa [2]. These strength values are at least two or three times higher than those of conventional aluminium alloys [3]. The notable characteristic of amorphous alloys containing more than 80 % at Al is that they can be completely bent through 180° without fracture and no appreciable cracking is observed [4]. Another useful property is their high corrosion resistance, but perhaps the most interesting aspect of the Al-based alloys is that they are low density, light-weight ma-

terials. All these properties taken together make bulk Al-based amorphous alloys promising candidates for structural applications. However, bulk amorphous samples usually face size limitations. It was reported that the maximum size of samples produced by rapid quenching only ranges from a few micrometers to a few centimeters [5]. Since the practical use of melt-quenched ribbons or rods for application is obviously limited, the feasibility to produce Al-based amorphous samples in the form of bulk sample was explored [6]. For that reason there were some attempts to produce bulk amorphous alloys by powder metallurgical processing methods. A remarkable characteristic of these systems is that the alloys contain more than 80 at. % of the basic component and do not show a deep eutectic, which has been a common guideline for easy glass formation. Instead, it appears that a multicomponent combination of constituents with large atomic size differences and a negative heat of mixing are key factors of glass formation. For amorphous Al alloys, glass formation is favoured for component composition

ranges of Al (80–92 at. %), rare earth (RE) (RE 3–20 at. %) and transition metal (TM) (1–15 at. %) [7, 8]. In this work, Al–La–Ni–Fe alloys of different compositions ( $\text{Al}_{82}\text{La}_{10}\text{Ni}_4\text{Fe}_4$ ,  $\text{Al}_{85}\text{La}_9\text{Ni}_3\text{Fe}_3$  and  $\text{Al}_{88}\text{La}_6\text{Ni}_3\text{Fe}_3$ ) were produced by ball-milling and investigated with respect to their microstructure and thermal stability. Subsequently, the first attempts were made to consolidate amorphous  $\text{Al}_{82}\text{La}_{10}\text{Ni}_4\text{Fe}_4$  powder using SPS.

## EXPERIMENTAL

Elemental Al, Fe, Ni and La powders (purity 99.9 %) were mixed to the nominal compositions of  $\text{Al}_{82}\text{La}_{10}\text{Fe}_4\text{Ni}_4$ ,  $\text{Al}_{85}\text{La}_9\text{Fe}_3\text{Ni}_3$  and  $\text{Al}_{88}\text{La}_6\text{Fe}_3\text{Ni}_3$  and canned into stainless steel vials with stainless steel balls at a powder to ball mass ratio of 10 : 200. To inhibit sticking of powder to the milling tools, 50 ml of hexane was used as a process control agent (PCA). The vials were evacuated and filled with protective Ar gas of  $3 \cdot 10^5$  Pa pressure. A high-energy planetary ball mill (AGO-2) was applied at a rotational speed of 300 rpm, where the vials were water-cooled. After milling, the powders were dried in a vacuum furnace at 80 °C. Microstructural characterization of milled and sintered samples was carried out by means of X-ray diffraction (XRD) (using  $\text{CuK}\alpha$  radiation), optical microscopy. The thermal stability of the alloys was characterized by differential scanning calorimetry (DSC) at 10 K/min under constant Ar flow. The compositions as well as the oxygen and carbon contents of milled samples were measured applying inductively coupled plasma spectroscopy (ICP) and carrier gas hot extraction. Consolidation of amorphous  $\text{Al}_{82}\text{La}_{10}\text{Fe}_4\text{Ni}_4$  powder was performed under high-vacuum condition in a spark-plasma sintering facility at a sintering temperature of 613 K, a heating rate of 10 K/min under 400 and 600 MPa.

## RESULTS AND DISCUSSION

X-ray diffraction analysis is a conventional technique for monitoring the progress of amorphization. X-ray diffraction patterns of mechanically alloyed  $\text{Al}_{88}\text{La}_6\text{Fe}_3\text{Ni}_3$  powders after 5, 50

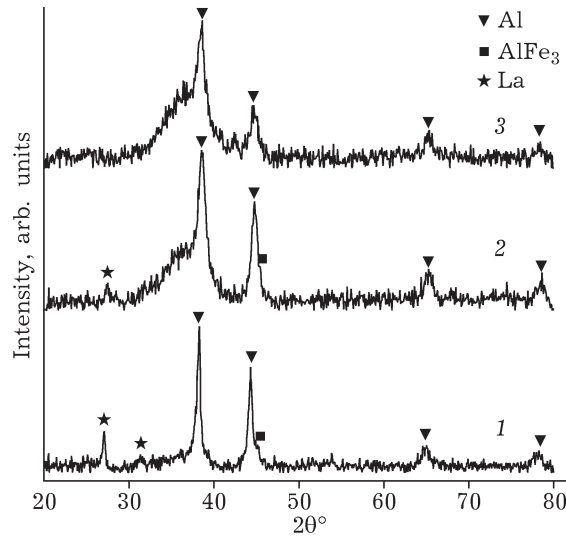


Fig. 1. XRD patterns of  $\text{Al}_{88}\text{La}_6\text{Fe}_3\text{Ni}_3$  powder milled for 5 (1), 50 (2), and 300 h (3).

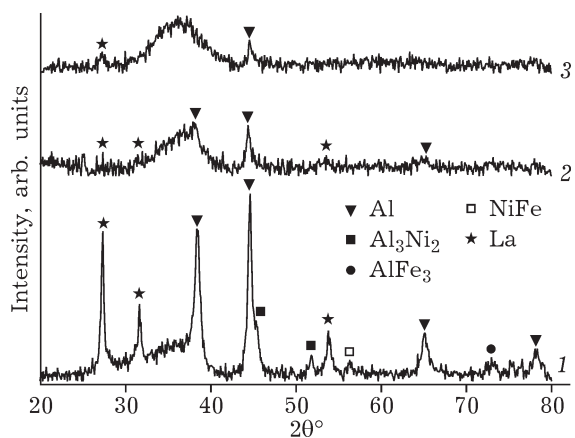


Fig. 2. XRD patterns of  $\text{Al}_{85}\text{La}_9\text{Ni}_3\text{Fe}_3$  powder milled for 5 (1), 50 (2), and 300 h (3).

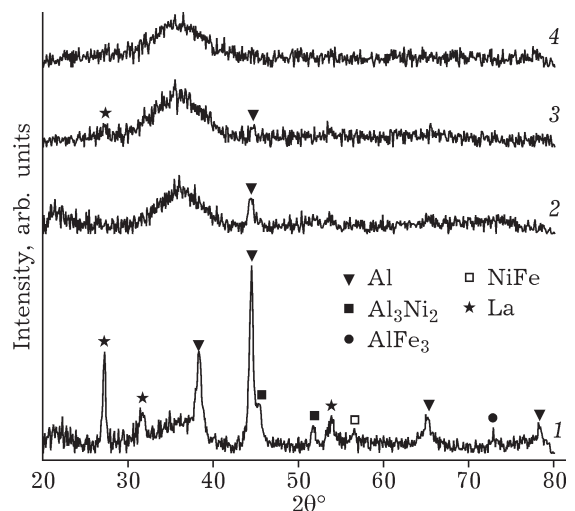


Fig. 3. XRD patterns of  $\text{Al}_{82}\text{La}_{10}\text{Fe}_4\text{Ni}_4$  powders milled for 5 (1), 50 (2), 300 (3), and 350 h (4).

and 300 h are given in Fig. 1. After 5 h of milling a broad halo peak can be recognized, indicating the beginning of the formation of the amorphous phase. After further milling for 50 h most of the material is amorphous and peaks of *fcc* Al, *hcp* La and intermetallic phase  $\text{AlFe}_3$  can be seen besides the broad halo peak. A few peaks belonging to *fcc* Al and *hcp* La phases still remained in amorphous matrix after 300 h milling.

Similar to the  $\text{Al}_{88}\text{La}_6\text{Fe}_3\text{Ni}_3$  alloy, the amorphization of  $\text{Al}_{85}\text{La}_9\text{Ni}_3\text{Fe}_3$  and  $\text{Al}_{82}\text{La}_{10}\text{Fe}_4\text{Ni}_4$  alloys set in after 5 h milling by the presence of the halo peak (Figs. 2, 3). A few peaks of *fcc* Al and *hcp* La are detected even after milling for 300 h for  $\text{Al}_{85}\text{La}_9\text{Ni}_3\text{Fe}_3$  whereas nearly fully amorphous structure can be obtained for  $\text{Al}_{82}\text{La}_{10}\text{Fe}_4\text{Ni}_4$  after 300 h milling. No distinct crystalline peaks can be seen in the XRD pattern of the powder milled for 350 h, suggesting that the sample is amorphous within the resolution of XRD. It is indicated by the XRD patterns that the glass-forming ability of the Al-La-Fe-Ni system increases with increasing La content and decreasing Al content. Such a tendency can be explained on the basis of the three empirical rules [9] applied for achieving large glass forming ability of rapidly quenched bulk metallic glasses, *i.e.* (1) multicomponent alloy systems consisting of more than three elements, (2) a significant atomic mismatch above

12 %, and (3) negative heat of mixing between constituent elements.

Values of atomic radii, atomic mismatch and heat of mixing for the Al-La-Fe-Ni system [10] are given in Table 1.

It is seen from Table 1 that La has the highest atomic radius as well as atomic radii mismatch with respect to the other elements. The size of Al also substantially differs from that of Fe and Ni. Furthermore, Al has high negative heat of mixing to Fe, Ni and La whereas La exhibits a positive mixing enthalpy with Fe. The latter should not be favourable for glass formation of rapidly quenched samples. However, Suryanarayana [11] reported that alloy systems with a positive heat of mixing also form an amorphous phase upon mechanical alloying. Therefore, the increasing size mismatch between the constituent elements with increasing La content may be the reason predominant for enhancement of the glass-forming ability.

Table 2 shows the oxygen and carbon content as well as chemical composition values for the mechanically alloyed amorphous powders. The measured compositions show a slight derivation from the nominal compositions due to sticking of powder to the milling tools. The oxygen content of the alloy powder is higher than 3 at. % and significant due to the long milling

TABLE 1

Atomic radii, atomic radius mismatch and enthalpies of mixing for Al-La-Fe-Ni systems

	Al	Fe	Ni	La
Al	–	11 %	13 %	24 %
Fe	–11 kJ/mol	–	2.2 %	34 %
Ni	–22 kJ/mol	–2 kJ/mol	–	34 %
La	–38 kJ/mol	5 kJ/mol	–27 kJ/mol	–
Atomic radius, nm	0.1432	0.1241	0.1246	0.1879

TABLE 2

Oxygen, carbon and chemical composition analysis for MA amorphous powders

Nominal composition	Measured composition	Oxygen content, at. %	Carbon content, at. %
$\text{Al}_{82}\text{La}_{10}\text{Fe}_4\text{Ni}_4$ (350 h MA)	$\text{Al}_{81.8}\text{La}_{9.9}\text{Fe}_{4.2}\text{Ni}_{4.1}$	6.82	3.43
$\text{Al}_{85}\text{La}_9\text{Fe}_3\text{Ni}_3$ (300 h MA)	$\text{Al}_{85.0}\text{La}_{8.9}\text{Fe}_{3.1}\text{Ni}_{3.0}$	3.1	2.6
$\text{Al}_{88}\text{La}_6\text{Ni}_3\text{Fe}_3$ (300 h MA)	$\text{Al}_{87.6}\text{La}_{6.0}\text{Fe}_{3.2}\text{Ni}_{3.2}$	3.3	2.5

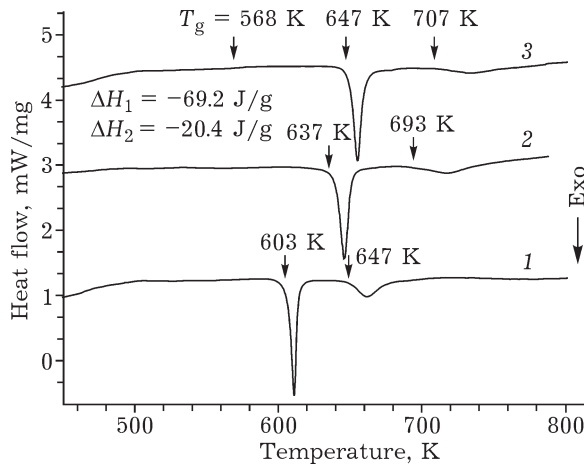


Fig. 4. DSC curves of mechanically alloyed  $\text{Al}_{82}\text{La}_{10}\text{Fe}_4\text{Ni}_4$  powders after 50 (1), 300 (2) and 350 h (3) of milling.

time. The high carbon content can be ascribed to the usage of hexane as a process controlling agent.

DSC measurements were done in order to investigate the thermal stability of the samples. It can be seen from Fig. 4 that the crystallization behaviour of  $\text{Al}_{82}\text{La}_{10}\text{Fe}_4\text{Ni}_4$  alloys milled for 50, 300 and 350 h takes place in two heat events. The glass transition and crystallization temperature and crystallization enthalpy values of  $\text{Al}_{82}\text{La}_{10}\text{Fe}_4\text{Ni}_4$  alloys are given in Fig. 4.

A shift of the exothermic peaks to higher temperatures can be observed if the milling time increases from 50 to 350 h. This can be explained by the fact that a significant amount of the *fcc* Al crystallites is still present in the amorphous matrix after 50 and 300 h. These crystallites serve as nucleation sites for crystallization. The onset temperature for primary crys-

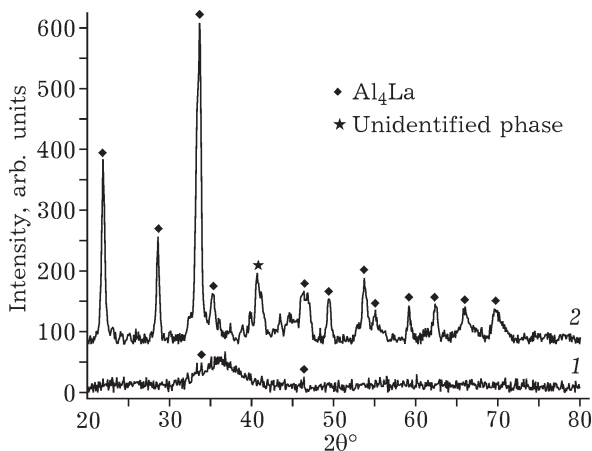


Fig. 5. XRD patterns of  $\text{Al}_{82}\text{La}_{10}\text{Fe}_4\text{Ni}_4$  after heat treatment at 643 (a) and 823 K (b) for 3 min.

tallization of the 350 h mechanically alloyed sample is 647 K and is higher than that reported for an amorphous alloy prepared by melt spinning [12]. In order to determine the crystallization behaviour of  $\text{Al}_{82}\text{La}_{10}\text{Fe}_4\text{Ni}_4$ , the alloy after 350 h of milling was annealed at peak temperature 643 and 823 K (Fig. 5).

The XRD pattern of the  $\text{Al}_{82}\text{La}_{10}\text{Fe}_4\text{Ni}_4$  alloy after annealing at 643 K for 3 min shows the peaks that can be indexed to intermetallic  $\text{Al}_4\text{La}$  phase. After heat treatment at 823 K a few new peaks can be observed. These peaks closely match those of intermetallic  $\text{Al}_4\text{La}$  and unidentified phases.

Figure 6 shows the optical micrographs of polished surface  $\text{Al}_{82}\text{La}_{10}\text{Fe}_4\text{Ni}_4$  samples sintered at 613 K under different pressure of 400 and 600 MPa. The highest relative density of  $\text{Al}_{82}\text{La}_{10}\text{Fe}_4\text{Ni}_4$  alloy can be obtained after sintering at 613 K and 600 MPa is about 96 %, as determined by image analysis of optical micrographs. The lack of complete densification can be ascribed to the low sintering temperature which was necessary to prevent crystallization. However, sintered samples are also par-

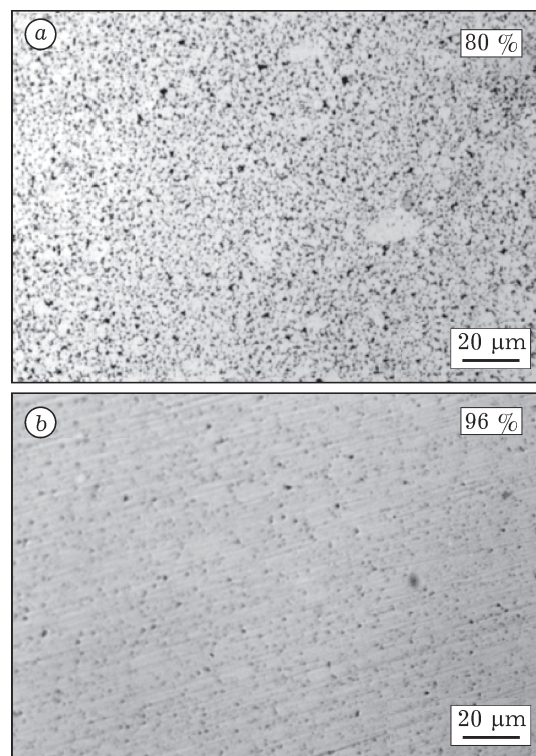


Fig. 6. Optical micrographs of the polished surface of  $\text{Al}_{82}\text{La}_{10}\text{Fe}_4\text{Ni}_4$  sintered at 613 K at a pressure of 400 (a) and 600 MPa (b).

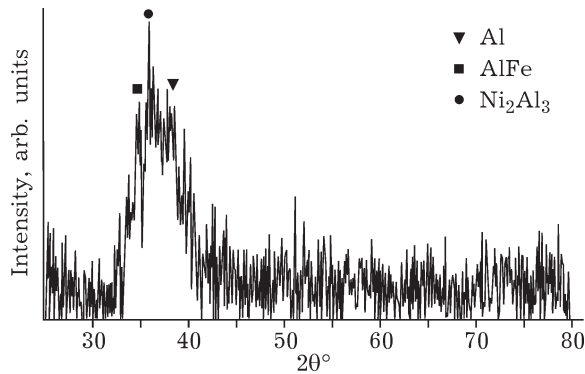


Fig. 7. XRD pattern of  $\text{Al}_{82}\text{La}_{10}\text{Fe}_4\text{Ni}_4$  sample sintered at 613 K and 600 MPa for 3 min.

tially crystallized even if sintering temperatures were chosen below onset crystallization temperatures. This can be explained by the fact that during sintering process the thermocouple was inserted at the border of sample. The temperature difference between the centre and border of the sample probably leads to peaks belonging to *fcc* Al,  $\text{Ni}_2\text{Al}_3$  and AlFe intermetallic phases occur in the XRD pattern (compare Fig. 7).

## CONCLUSIONS

Amorphous  $\text{Al}_{82}\text{La}_{10}\text{Ni}_4\text{Fe}_4$ ,  $\text{Al}_{85}\text{La}_9\text{Ni}_3\text{Fe}_3$  and  $\text{Al}_{88}\text{La}_6\text{Ni}_3\text{Fe}_3$  alloy powders were produced by MA. Fully amorphous structure was obtained for  $\text{Al}_{82}\text{La}_{10}\text{Ni}_4\text{Fe}_4$  after 350 h MA within the resolution of the XRD method. Similar to melt-

spun samples, the glass forming ability for the Al–La–Fe–Ni system increases with adding La content due to increasing atomic radii mismatch between constituent element. The highest relative densities of  $\text{Al}_{82}\text{La}_{10}\text{Fe}_4\text{Ni}_4$  sample is 96 % and partly amorphous structure retains after sintering due to a different temperature between the edge and centre of sample. It is needed to optimize sintering parameters to get fully amorphous structure and full density of  $\text{Al}_{82}\text{La}_{10}\text{Fe}_4\text{Ni}_4$  alloy in the future work.

## REFERENCES

- 1 N. Bassim, C. S. Kiminami, M. J. Kaufman *et al.*, *Mat. Sci. Eng. A*, 304–306 (2001) 332.
- 2 A. Inoue, H. M. Kimura, K. Sasamori and T. Masumoto, *Ibid.*, 217/218 (1996) 401.
- 3 M. Gogebakan, P. J. Warren, B. Cantor, *Ibid.*, 226–228 (1997) 168.
- 4 A. Inoue, *Prog. Mat. Sci.*, 43 (1998) 365.
- 5 J. F. Loffler, *Intermetallics*, 11 (2003) 529.
- 6 M. Calin, H. Grahl, M. Adam *et al.*, *J. Mat. Sci.*, 39 (2004) 5295.
- 7 J. H. Perepezko, R. J. Hebert, W. S. Tong, *Intermetallics*, 10 (2002) 1079.
- 8 A. Inoue, H. Kimura, High-Strength Al-Based Nanostructure Alloys.
- 9 Y. C. Kim, S. Yi, W. T. Kim and D. H. Kim, *Mat. Sci.*, 360–362 (2001) 67.
- 10 W. H. Wanga, C. Dongb and C. H. She, *Ibid.*, 28 (1990) 407.
- 11 C. Suryanarayana, *Prog. Mat. Sci.*, 46 (2001) 1.
- 12 Joysurya Basu and S. Ranganathan, *Intermetallics*, 12 (2004) 1045.